Available online at www.sciencedirect.com

SciVerse ScienceDirect

journal homepage: www.elsevier.com/locate/he

Cobalt-free composite cathode for SOFCs: Brownmillerite-type calcium ferrite and gadolinium-doped ceria

*Seung Jun Lee, Seok-Min Yong, Dong Seok Kim, Do Kyung Kim**

Department of Materials Science and Engineering, Korea Advanced Institute of Science and Technology (KAIST), 291 Daehak-ro, Yuseong-gu, Daejeon 305-701, Republic of Korea

ARTICLE INFO

Article history:
Received 8 June 2012
Received in revised form
10 August 2012
Accepted 23 August 2012
Available online 21 September 2012

Keywords:
$Ca_2Fe_2O_5$
SOFCs
Composite cathode
Co-free cathode
Electrochemical performance

ABSTRACT

A cobalt-free composite $Ca_2Fe_2O_5$ (CFO) − $Ce_{0.9}Gd_{0.1}O_{1.95}$ (GDC) is investigated as a new cathode material for intermediate-temperature solid oxide fuel cells (IT-SOFCs) based on a $Gd_{0.1}Ce_{0.9}O_{1.95}$ (GDC) electrolyte. The cathodes had brownmillerite structure with x wt.% $Gd_{0.1}Ce_{0.9}O_{1.95}$ (GDC) − (100−x) wt.% $Ca_2Fe_2O_5$ (CFO), where x = 0, 10, 20, 30 and 40. The effect of GDC incorporation on the thermal expansion coefficient (TEC), electrochemical properties and thermal stability of the CFO–GDC composites is investigated. The composite cathode of 30 wt.% GDC − 70 wt.% CFO (CG30) coated on $Gd_{0.1}Ce_{0.9}O_{1.95}$ electrolyte showed the lowest area specific resistance (ASR), 0.294 Ω cm^2 at 700 °C and 0.122 Ω cm^2 at 750 °C. The TEC of the CG30 cathode was 13.1 × 10^{-6} $°C^{-1}$ up to 900 °C, which is a lower value than for CFO alone (13.8 × 10^{-6} $°C^{-1}$). Long-term thermal stability and thermal cycle testing of CG30 cathodes were performed. Stable ARS values were observed during both tests without delamination at the cathode–electrolyte interface. An electrolyte-supported single cell with a 300-μm-thick GDC electrolyte and an anode-supported single cell with ~10-μm-thick yttria-stabilized zirconia (YSZ) with a GDC buffer layer attained maximum power densities of 395 mW cm^{-2} at 750 °C and 842 mW cm^{-2} at 800 °C, respectively. The unique composite composition of CG30 demonstrates enhanced electrochemical performance and good thermal stability for IT-SOFCs.

1. Introduction

Solid oxide fuel cells (SOFCs) are electrochemical energy conversion devices characterized by high working efficiency, low pollution and fuel flexibility [1–4]. Currently, one of the main issues for the development of SOFCs involves lowering operating temperatures to the intermediate temperature range of 600–800 °C. In the intermediate temperature region (600–800 °C), however, the cathode becomes the limiting factor in determining the overall cell performance because the cathode's electrochemical activity dramatically decreases with decreasing temperature [4,5].

For SOFCs, $La_{1-x}Sr_xMnO_{3-\delta}$ (LSM) is widely investigated as a potential cathode material [3,6,7]. LSM is characterized by high and purely electronic conductivity. Because LSM has low ionic conductivity, the oxygen-reduction is restricted at the cathode–electrolyte interface. Therefore, reducing the operating temperature makes the performance of purely electronic conducting cathode decrease rapidly. Cobalt-based perovskite materials, such as LSCF [8] and BSCF [9],

* *Corresponding author*. Tel.: +82 42 350 4118; fax: +82 42 350 3310.
E-mail address: dkkim@kaist.ac.kr (D.K. Kim).

0360-3199/$ – see front matter
http://dx.doi.org/10.1016/j.ijhydene.2012.08.100

demonstrate mixed ionic and electronic conducting behavior, and thus, oxygen reduction occurs along the cathode material's entire surface. Therefore, cobalt-based cathodes exhibit higher electro-catalytic performance at reduced temperatures. Unfortunately, cobalt-based cathode materials demonstrate high thermal expansion behavior compared to electrolyte materials because of the generation of oxygen vacancies and a low-spin to high-spin transition of Co^{3+} [2–4]. In addition, cobalt-based cathode materials have drawbacks, such as high chemical reactivity with electrolyte materials, cobalt evaporation and the high cost of elemental cobalt [2,3,5,10–13]. Iron-based perovskite oxides like doped $SrFeO_{3-\delta}$, however, could well serve as promising alternative to cobalt-based cathode materials, because of the less flexible redox behavior and low price of iron [14,15].

$Ca_2Fe_2O_5$ is a member of the family of compounds with the general formula $A_2B_2O_5$ (A = Ca, Sr; B = Fe, Co) [16–21]. The physical properties of $Ca_2Fe_2O_5$, such as electronic and oxygen-ionic transport, thermoelectric properties and catalytic and photocatalytic behavior, have been studied [17,22–24]. CFO's brownmillerite structure consists of alternating perovskite layers of corner-sharing FeO_6 octahedra and FeO_4 tetrahedra [17,19]. The structure is often classified as an oxygen-deficient perovskite where the oxygen vacancies ordered along (010) planes contribute to ionic conductivity, forming one-dimensional oxygen ion migration in the tetrahedral layers and contributing to the material's fast oxygen ionic conductivity [17–19]. Recently, the mixed ionic-electronic conductive properties of brownmillerite-type structure materials have begun to be investigated [25].

In addition, $Ca_2Fe_2O_5$ has the advantage of a low thermal expansion coefficient (TEC) of $13.1 \times 10^{-6}{}^{\circ}C^{-1}$ in the range of 373–953 K [17], which provides good thermal expansion compatibility with electrolyte materials such as GDC and YSZ. Consequently, $Ca_2Fe_2O_5$ can be potentially utilized as a cathode material for IT-SOFCs because of its mixed ionic–electronic conducting properties and a thermal expansion coefficient similar to those of electrolyte materials. To date, however, few reports of the use of $Ca_2Fe_2O_5$ as a potential cathode material have been published.

One commonly used means for improving cathode performance is to add an ionically conducting second phase to the electrode material to form a composite cathode [1,2,4,5,7]. The addition of a highly ionic conductive phase to the electrode layer is effective in improving the cathode's electrocatalytic activity due to enlargement of the electrochemically active area, i.e., the triple phase boundary (TPB) and the creation of ionic conducting path due to the high ionic conductivity. With the aim of improving the electrocatalytic activity of $Ca_2Fe_2O_5$ and achieving a match between the thermal expansion coefficients of the electrolyte and the cathode, we investigated the electrochemical properties and thermal expansion behavior of $Ca_2Fe_2O_5$ and GDC composite cathodes.

2. Experiment procedure

A brownmillerite $Ca_2Fe_2O_5$ (CFO) was synthesized via a citrate combustion method, and composite cathodes were synthesized via a precipitation method. Analytical grade $Ca(NO_3)_2{\cdot}4H_2O$ (>99.9%) and $Fe(NO_3)_3{\cdot}9H_2O$ were used as precursors for the synthesis of oxide powders, and citric acid ($C_6H_8O_7$) (99%) was used as fuel for the combustion reaction.

Initially, stoichiometric amounts of the precursors were dissolved in deionized water with constant stirring, and then citric acid was added to the clear solution. The resultant transparent solution was heated at 70 °C until sufficient water had evaporated, resulting in a transparent gel. The gel was heated at 125 °C in an oven for 24 h. The dried gel was pre-fired at 250 °C and subsequently calcined at 500 °C for 4 h and 900 °C for 10 h to yield the desired crystalline oxide powders.

The stoichiometric amounts of $Ce(NO_3)_3{\cdot}6H_2O$ (99.9%) and $Gd(NO_3)_3{\cdot}6H_2O$ (99.9%) were dissolved in 50 ml of ethanol to form the calculated x wt.% $Ce_{0.9}Gd_{0.1}O_{1.95}$ in composite. To the above clear solution, (100−x) wt.% of calcined CFO powder was dispersed under sonication for 2 h. The $(C_2H_5)_2NH$ (diethylamine, 99.9%) precipitant was used to precipitate the GDC in the presence of CFO to form the composite. The obtained composite powders were dried at 80 °C for 12 h and calcined at 900 °C for 10 h. The CFO–GDC composites had a composition varying from 0 to 40 wt.%, and the designations of these cathodes are summarized in Table 1.

The phases of the synthesized powders were characterized with a third-generation synchrotron powder X-ray diffractometer (XRD) from the 8C2 station beam line with Cu-K_α radiation (λ = 1.549 Å) at the Pohang Light Source (PLS) in Korea. The diffraction data were collected in the 10- to 130-degree ranges (2θ) at a step of 0.01°. The cross-sectional microstructures of the cells were inspected with a scanning electron microscope (FE-SEM Philips XL30 FEG).

Rectangular-shaped bars with dimensions of 3 mm × 3 mm × 12 mm were sintered at 1100 °C for 5 h in air and were used for TEC measurement. TECs of the sintered samples were measured using a Netzsch DIL 402C dilatometer at temperatures between 30 and 900 °C at a heating rate of 5 °C min^{-1} in air.

The symmetrical half-cells were fabricated by screen-printing. The as-fabricated half-cells were sintered at 1000 °C for 2 h in air to form an effective cathode surface area of 0.385 cm^2 and thickness of ~18 μm. Platinum paste (ESL) was applied to the edge of the same side of the working electrode on the electrolyte to act as a reference electrode. The area specific resistances (ASRs) were measured via 3-probe AC impedance spectroscopy (Solartron 1260 impedance/Gain-phase analyzer) as a function of temperature (550–800 C) in flowing air.

Table 1 – Chemical compositions and their designations.

Chemical composition	Designation
$Ca_2Fe_2O_5$	CFO (CG0)
$Gd_{0.1}Ce_{0.9}O_{1.95}$	GDC
10 wt.% GDC and 90 wt.% $Ca_2Fe_2O_5$	CG10
20 wt.% GDC and 80 wt.% $Ca_2Fe_2O_5$	CG20
30 wt.% GDC and 70 wt.% $Ca_2Fe_2O_5$	CG30
40 wt.% GDC and 60 wt.% $Ca_2Fe_2O_5$	CG40

Electrolyte-supported single cells with 300-μm of GDC as the electrolyte as well as anode-supported single-cells with 10-μm of YSZ as the electrolyte and GDC as the buffer layer were fabricated using a screen-printing method. A source meter (Keithley 2400) was used to measure the *I*–*V* polarization under flowing humidified H_2 (~3% H_2O) as a fuel and in air as an oxidant at a rate of 100 sccm.

3. Results and discussion

The synchrotron source XRD patterns of the CFO (CG0) and CG30 cathodes calcined at 900 °C for 10 h are presented in Fig. 1. The XRD pattern of CFO is evidence of a single-phase, high crystalline brownmillerite structure (space group Pnma, No. 47-1744) without any impurity phase; CFO's indexed primary peaks are summarized in Fig. 1. The unit cell parameters for CFO were $a = 5.426$ Å, $b = 14.764$ Å and $c = 5.598$ Å, and the cell volume was 444.453 Å^3. The patterns of the CG30 composite show the presence of indexed peaks corresponding to GDC and CFO without any other secondary phases. This indicates that CFO has a good chemical compatibility with GDC electrolytes below 900 °C, supporting its use as a cathode in SOFCs.

Thermal stress from the difference in the TECs of adjacent cell components may result in detachment of the interface between layers during the repeated thermal cycling operation [5,26]. Moreover, the thermal expansion incompatibility can cause thermal stress in SOFCs and thus result in poor long-term thermal stability performance [4,5]. Therefore, it is important to improve the thermal expansion compatibility between the cathode and the electrolyte. Fig. 2 shows the thermal expansion curves for different wt.% CG composite cathodes, and the table in the inset shows the calculated TEC values from the plots, which exhibit the relatively reduced TEC of CFO (13.8×10^{-6} °C^{-1}) compared with cobalt-based cathode materials [27,29]. As expected, a further decrease in

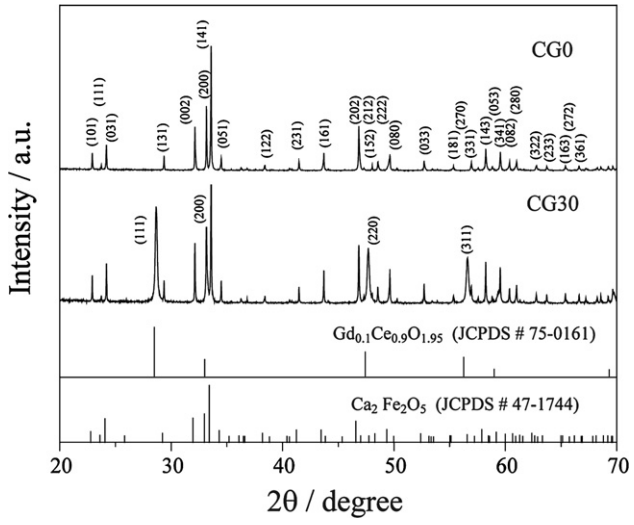

Fig. 1 – Synchrotron XRD patterns of the $CaFe_2O_5$ (CG0) and CG30 powders calcined at 900 °C for 10 h and compared with the JCPDS data.

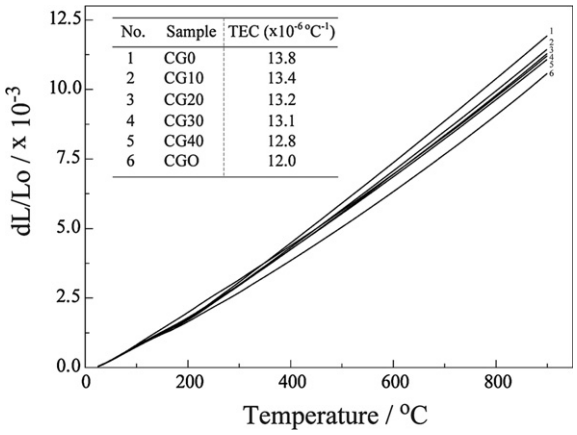

Fig. 2 – Thermal expansion curves (dL/L_0) of CG composites in the temperature range of 30–900 °C in air. Inset table shows the TEC values for CG composites.

the TEC values was observed with the addition of GDC into CFO. The TEC of CG0 decreased to 13.1×10^{-6} °C^{-1} for the CG30 cathode. The reduced TEC is mainly attributed to GDC's smaller TEC. This value is compatible with the GDC electrolyte (TEC is 12.0×10^{-6} °C^{-1}) compared to the TEC value of cobalt-based LSCF [27] and GBCO [29]. Thus, the addition of GDC led to a decrease in the thermal expansion coefficient, which improved the thermal stability of the CG30 cathode analyzed in the later sections.

Impedance spectra for the CFO cathode with respect to various sintering temperatures are shown in Fig. 3 (a). The ohmic resistance was removed in the impedance spectra in order to compare the polarization resistance of the cathode. The cathode sintered at 1000 °C showed the lowest cathodic polarization resistance of 1.934 Ω cm^2 at 650 °C. Fig. 3 (b) clearly reveals that the cathode sintered at 1000 °C possessed the lowest ASR values at various temperatures.

Generally, cathode materials have fine grain size, a large surface area and sufficient porosity as well as demonstrate good adhesion between the cathode and electrolyte to obtain high electrode performance [27]. However, for the cathode sintered at 900 °C (data not shown), weak interconnectivity between the CFO and electrolyte was observed. The weak connection between agglomerated particles will increase the resistance of bulk-surface diffusion of oxygen species as well as increase electron transfer through the porous cathode. Therefore, the sintering temperature must be increased to enable the formation of good connections between the CFO particles. At 1100 °C and 1200 °C, improved contact between the cathode materials was observed. However, cathodes sintered at temperatures higher than 1100 °C demonstrated large areas of dense regions with few micro-pores. These effects decreased the electrode porosity and active sites for oxygen reduction because of the growth of cathode particles, resulting in an increase of ASR.

In summary, it can be concluded that a sintering temperature of 1000 °C provides the best balance between the conflicting electrode requirements of maintaining a porous, high surface area structure while simultaneously providing a strong, well-sintered and adherent layer. At 900 °C, the

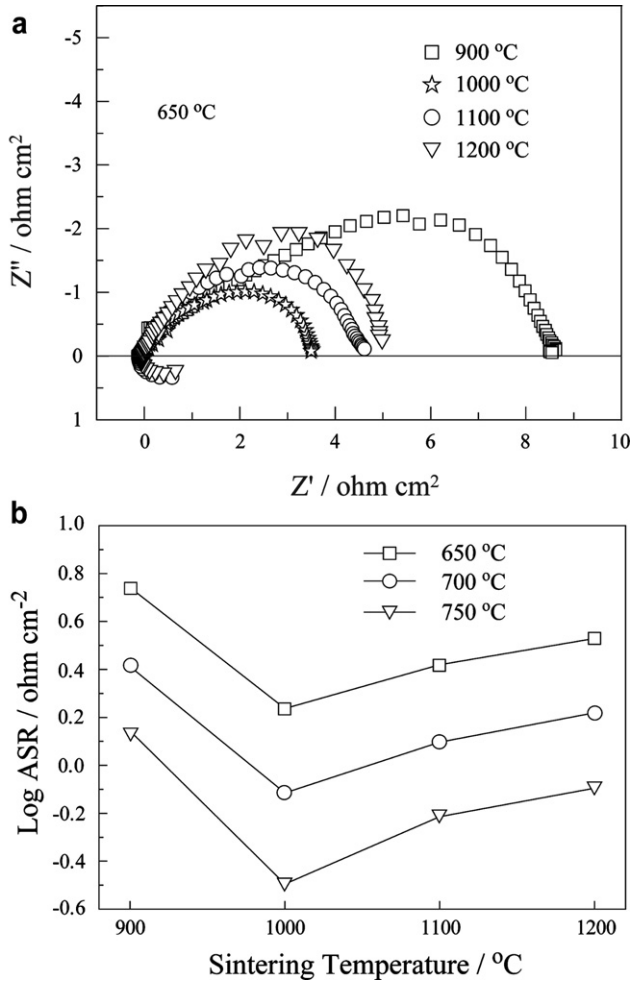

Fig. 3 – (a) AC impedance spectra measured at 650 °C in air for $Ca_2Fe_2O_5$ cathode sintered at different temperature. (b) Area specific resistance values from 650 to 750 °C as a function of sintering temperature.

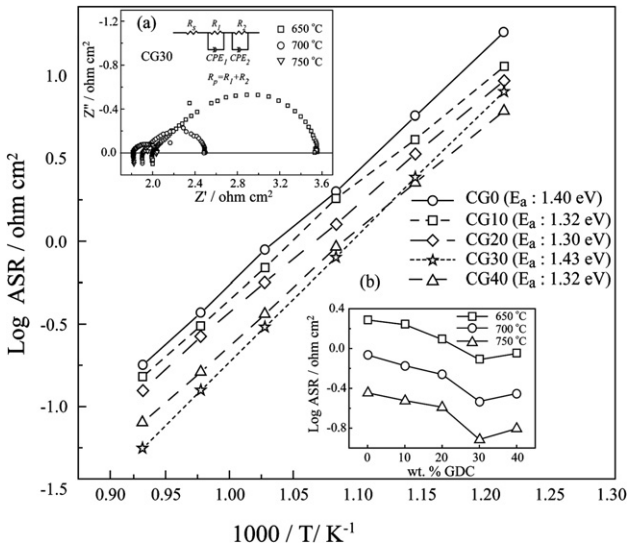

Fig. 4 – Arrhenius plots of log ASR for the symmetrical cells of different wt.% CG/GDC at interface, measured in air. The inset (a) shows impedance spectrum for the symmetrical cell fabricated with CG30 cathode on the GDC electrolyte. The inset (b) shows the ASR values *vs.* wt.% of composite electrodes.

temperature is not high enough to provide a structure of sufficient particle necking for good contact and adhesion. At higher temperatures, however, the reduced surface area caused by the densification of the cathode regions results in a decrease in the active site for oxygen reduction [28,30]. Based on the ASR values, the following experiments were sintered at 1000 °C for composite cathodes.

The calculated ASR values of the different wt.% CG composites from the interface resistances of the impedance spectra are shown in Fig. 4. The inset (a) in Fig. 4 shows a typical impedance spectrum for the symmetrical cells fabricated with the CG30 cathode onto the GDC electrolytes, measured at 650, 700 and 750 °C. The resistivity ($R_p = R_1 + R_2$) was obtained by fitting the impedance spectrum with an equivalent circuit model (inset (a) in Fig. 4) using the nonlinear least squares fitting program of the Z-View software. The intercept of the semicircle on the real axis in the high-frequency region represents the total ohmic resistivity (R_s) of the electrolyte. The radius of the arc between the two intercepts in the high- and low-frequency regions on the real axis corresponds to the polarization resistivity (R_p) of the cathodes.

As shown in inset (a), both the ohmic resistance and electrode resistance decrease with an increase in measuring temperature. The inset (b) in Fig. 4 shows the plot of ASR values *vs.* different wt.% CG composites. R_p decreased with an increase in GDC content, reaching a minimum at a GDC content of 30 wt.% but increasing with a further increase in GDC. In Fig. 4, the CG30 composite cathode on the GDC electrolyte showed an ASR value of 0.294 Ω cm^2 at 700 °C, which is lower than the value for the CG0 cathode (0.860 Ω cm^2 at 700 °C). The ASR values are higher than that of cobaltite cathode but quite compatible with previously reported cobalt-free cathode [9,14,15,29]. The inset (b) clearly reveals that the CG30 composite possessed the lowest ASR values at various temperatures. A further increase in GDC content to a value higher than 30 wt.% resulted in a higher interfacial polarization resistance.

Generally, the addition of a highly conductive phase to the electrode, i.e., composite cathodes, is effective in expanding the electrochemical reaction zone from the limits of the two-dimensional interface between the electrolyte and the cathode to the cathode's entire area. It is believed that the ionically conducting GDC, when added to a cathode, can extend the electrochemically active reaction zone from the triple phase boundaries at the two-dimensional interface between the electrolyte and the cathode to the three-dimensional bulk of the electrode [1,2,4,5,7]. As a result, the addition of the high ionic conductive GDC in CFO–GDC composite cathodes may extend the triple-phase boundaries, resulting in much lower overpotentials toward oxygen reduction by providing the short-circuit paths for ion transport. These effects reflect a decrease in cathode polarization caused by a reduction in charge transfer resistance [1,2,4,7]. In addition to increased TPBs, the addition of an ionically

conducting phase also increases the total concentration of oxygen vacancies, improving the adsorption of oxygen gas and the diffusion of oxygen ions in the electrode, which results in a reduction in the diffusion-related process [7].

Fig. 5 (a) and (b) show the cross-sectional views of an interface between the CG30 cathode and the GDC electrolyte after half-cell testing. The SEM images show thin layers of cathodes (~18 μm) with a highly porous morphology that ensured good gas diffusion. The images also display the presence of inter-connectivity at the interfaces between the CG30 cathode and GDC electrolyte. Fig. 5 (b) shows that the composite cathode consisted of homogeneously distributed, nano-sized (~100 nm) GDC particles (indicated by arrows) on the surface of the CFO particles. In addition, the GDC particles on the large CFO particles adhered to the dense GDC electrolyte. This typical morphology may account for reduced cathode polarization resistance during the oxygen reduction reaction. This suggests an explanation for enhancement of the electrochemical properties of the CG30 cathode compared with those of the pure CG0 cathode.

To evaluate the thermal stability of the CG30 cathode, the ASRs of the half-cell as a function of thermal cycling and long-term thermal stability were surveyed using AC impedance spectroscopy (Fig. 6), and the results are shown in Fig. 7. The half-cell was thermally cycled 50 times between 200 and 650 °C, with heating and cooling rates of 5 °C/min, as shown in inset (b) of Fig. 7. In addition, the long-term stability test was performed at 650 °C for 500 h, and ASR was measured every 12 h. Typical impedance spectra of delaminated cells showed increases in both the ohmic resistance and the diameter of electrode arcs [26]. In this research, however, the impedance spectra of cyclic tests (after the 5th and 50th tests) and long-term stability tests (after 120 h and 500 h) represent similar ohmic resistance and electrode resistance. This result indicated that the GG30 cathode showed superior thermal stability without any delamination between the cathode and electrolyte during the thermal stability test.

In accordance with impedance spectra analysis, small or negligible changes in polarization resistance were observed after 50 thermal cycles, as shown in Fig. 7. The CG30 cathode also demonstrated stable performance for 500 h at 650 °C in light of changes in the ASR value. Two insets in Fig. 7 (a) and (c) show the cross-sectional views of the interface between the CG30 cathode and the GDC electrolyte after the cell tests. The

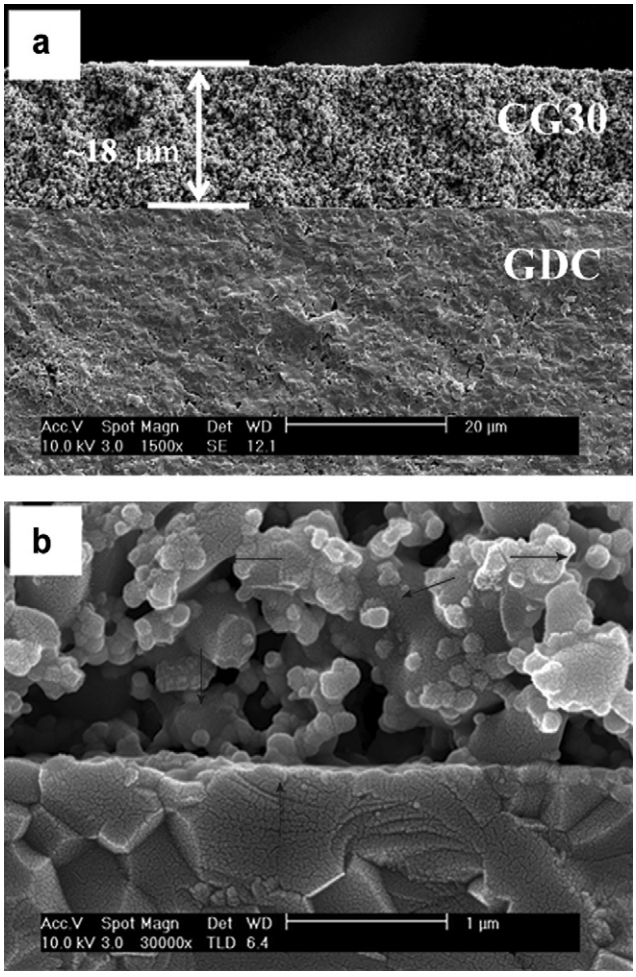

Fig. 5 – SEM images of the cross-section of an interface between the CG30 cathode and GDC electrolyte substrate (a) low-magnification and (b) high-magnification after cell test.

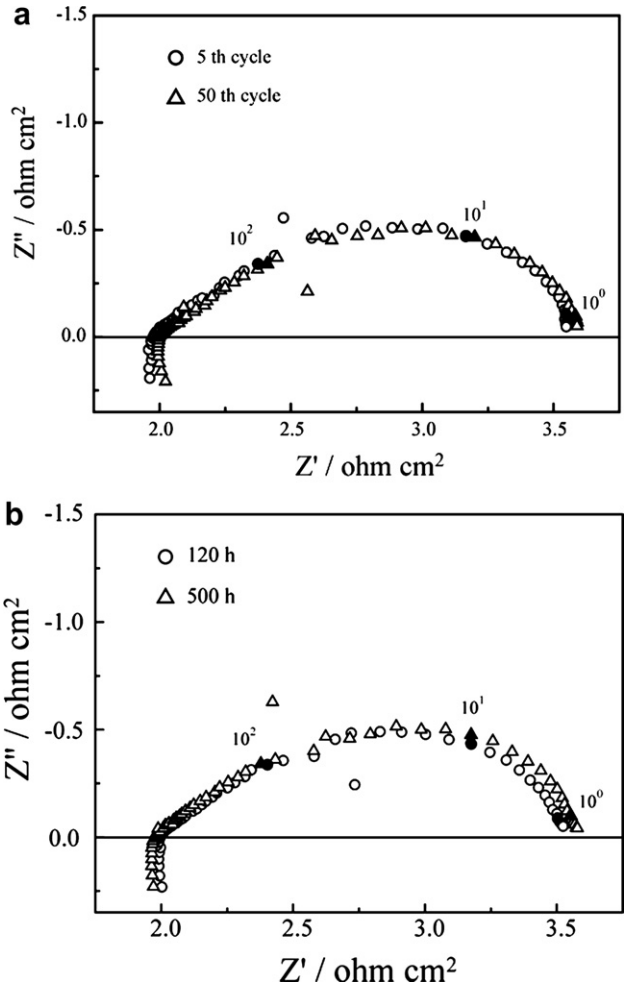

Fig. 6 – Impedance spectra of a CG30 cathode of (a) 5th cycle and 50th cycle at the temperature range of 200 and 650 °C and (b) at 120 h and 500 h of operation at 650 °C.

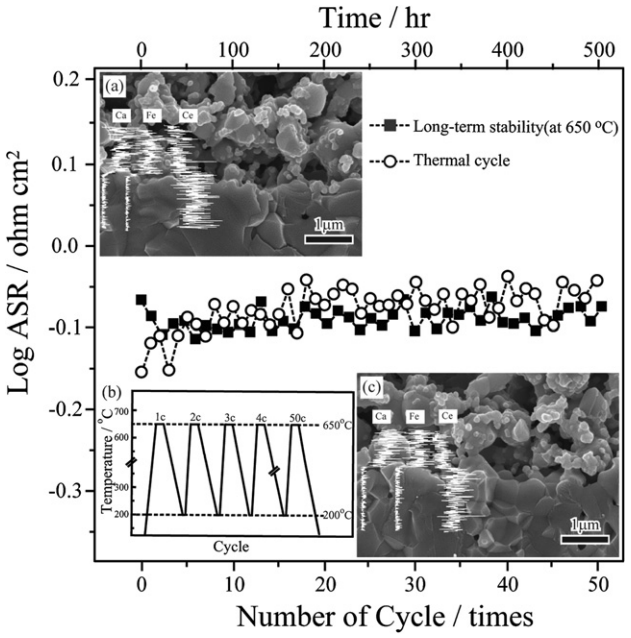

Fig. 7 – ASR values of CS30 at 650 °C under flowing air for long-term thermal stability, thermal cycle result. Inset (a) and (c) shows SEM images with EDS line profiles at the interface between cathode and electrolyte after cycle test and long-term thermal stability, respectively. And inset (b) shows temperature patterns for the thermal cycle test.

SEM micrographs revealed high porosity and good connectivity without cracking or delamination, which led to the stable polarization resistance during the cell test. The elemental line profiles on the SEM image in insets (a) and (c) exposed the density of elements Ce, Ca and Fe in the cathode and electrolyte regions. These results confirmed the presence of elements in the limited regions without any penetration of elements during the thermal stability test.

Fig. 8 shows the electrochemical performances of the electrolyte-supported single-cell configuration of CG/~300 μm GDC/Ni–GDC in the temperature range of 650–750 °C using humidified H_2 (~3% H_2O) as a fuel and air as an oxidant. The open circuit voltage (OCV) was lower than 1.0 V and increased with decreasing temperature. The decrease of the OCV was induced by electronic conduction in the GDC electrolyte caused by the reduction of Ce^{4+} to Ce^{3+}. The maximum power density of CG0 was 250 mW cm^{-2}, and that of CG30 was 395 mW cm^{-2} at 750 °C. These results demonstrate that the CG30 cathode exhibited high performance in the intermediate-temperature regime, which was compatible with the data reported in the literature for cobalt-free cathode materials [12,13,31].

YSZ has been widely used as an electrolyte in solid oxide fuel cells. In this research, a single-cell test onto the YSZ electrolyte was also investigated. Prior to the single-cell test with the YSZ electrolyte, a chemical compatibility test between the cathode and YSZ electrolyte was performed using XRD. The results are shown in Fig. 9, which shows XRD patterns after heating the mixture of CFO and YSZ from 700 to 1000 °C for 1 h. A reaction between CFO and YSZ occurs 800 °C

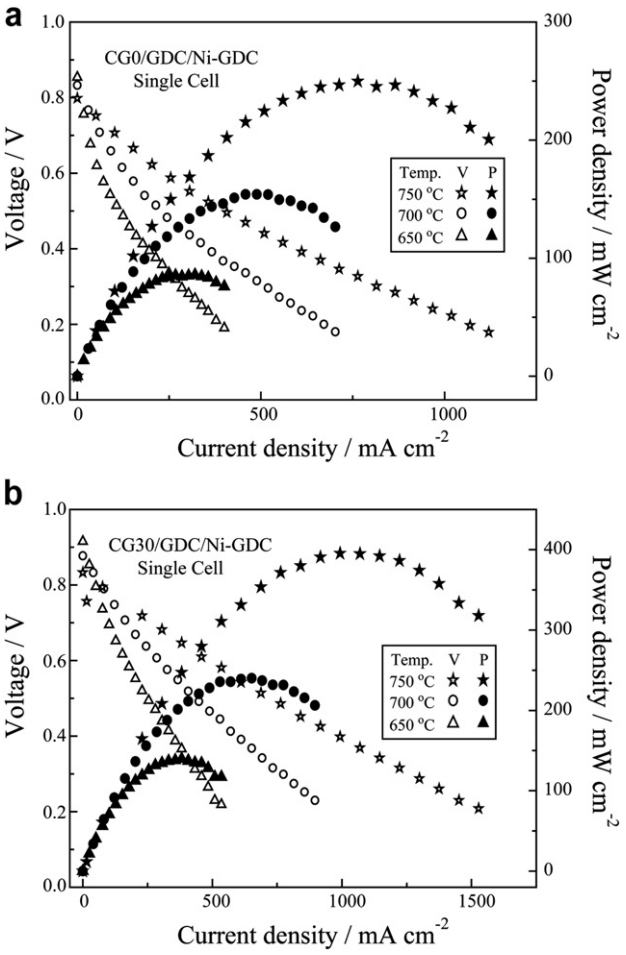

Fig. 8 – Electrochemical performance of CG0 and CG30/GDC/Ni–GDC single-cells under humidified H_2 fuel and air oxidant at different temperatures.

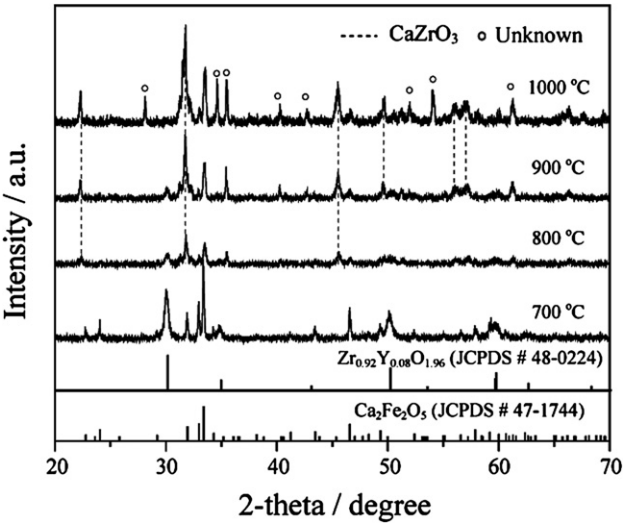

Fig. 9 – X-ray powder diffraction patterns of $Ca_2Fe_2O_5$ and YSZ mixture after heat-treated at the temperature range of 700 and 1000 °C for 2 h. The dot lines correspond to $CaZrO_3$ and are the secondary phase between $Ca_2Fe_2O_5$ and YSZ. The open circle is an unknown phase.

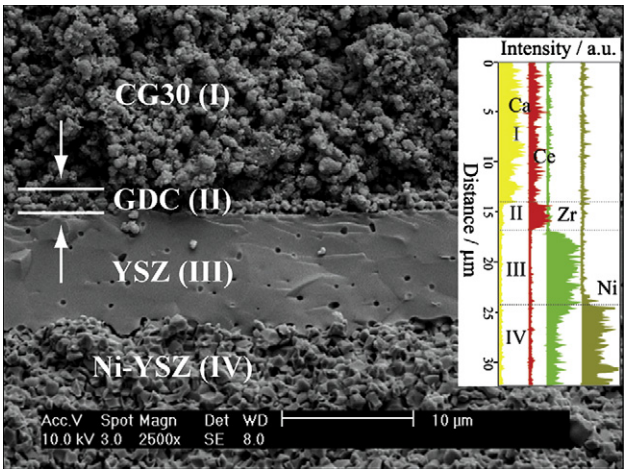

Fig. 10 – SEM image of anode-supported single cell configuration of CG30/YSZ/Ni–YSZ with ~3 μm GDC buffer layer fabricated 1000 °C for 2 h.

and formed $CaZrO_3$ (JCPCS #35-0790) of unknown phase. This indicates that CFO was therefore unsuitable as a cathode in direct contact with the YSZ electrolyte where temperatures exceed 800 °C. To prevent side reactions at the cathode and electrolyte interface, ~3 μm GDC buffer layers at 1250 °C for 2 h were prepared onto the cathode side of the YSZ electrolyte.

Fig. 10 shows the cross-sectional SEM image of the anode-supported singe cell, which was sintered at 1000 °C for 2 h. The middle of the SEM image indicates the porous GDC buffer layer (~3 μm)/dense YSZ (~10 μm) electrolyte with a total thickness of ~13 μm, and each side of the electrolyte film shows the anode and cathode. The EDS line profiles corresponded well with the chemical compositions of the different layers and ensured the absence of delamination or inter-diffusion between the cell components.

Fig. 11 shows the electrochemical performances of the anode-supported single-cell configuration of CG30/~10 μm YSZ/Ni–YSZ with GDC buffer layer in the temperature range of 700–800 °C. The open circuit voltage showed higher values

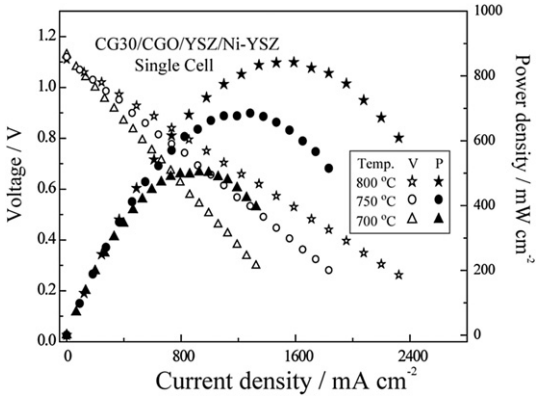

Fig. 11 – Electrochemical performance of CG30/YSZ/Ni–YSZ single-cells with ~3 μm GDC buffer layer under humidified H_2 fuel and air oxidant in the temperature range of 700–800 °C.

than those for the GDC electrolyte. The measured open circuit voltage at 800, 750 and 700 °C were 1.11, 1.12 and 1.13 V, respectively. The maximum power density of CG30 was 842 mW cm^{-2} at 800 °C, which is higher than the value for the GDC electrolyte. The enhanced power density might have a greater decrease in the ohmic resistance-related oxygen ion diffusion through the ~10-μm YSZ electrolyte than for the ~300-μm GDC electrolyte. Therefore, the CG30 cathode exhibited high performance in the intermediate-temperature regime on both the GDC and YSZ electrolytes.

In summary, it can be concluded that the enhanced electrochemical performance and structural stability of the CG30 cathode was due to the addition of the GDC to the CFO, which yielded a large triple-phase boundary and provided short routes for ion transport for mixed conducting materials that are advantageous for efficient oxygen reduction processes and fast charge transport [7]. The addition of GDC also affected the good interconnectivity between the composite particles and the interface of the cathode and electrolyte because of the reduced TEC.

4. Conclusions

In the present study, a series of cobalt-free $Ca_2Fe_2O_5$ and composite cathodes with GDC were employed as the cathodes for SOFCs. The different weight percentages of CG0 to CG40 composite cathodes were synthesized via the citrate combustion method followed by the precipitation method. The TEC values were reduced by mixing GDC and $Ca_2Fe_2O_5$ particles to form CFO–GDC composite cathodes, which significantly improved the thermal stability of the CG30 cathode by achieving a match of the TEC between the electrolyte and cathode. Among the CG composite cathodes, the CG30 cathode exhibited the best performance. The improved performance of $Ca_2Fe_2O_5$–GDC composite electrodes is due to a combination of the decrease in the charge transfer and the diffusion-related resistance by the addition of high ionic conductive GDC in the cathode. The maximum power density of the electrolyte-supported and anode-supported single-cell delivered 395 mW cm^{-2} at 750 °C and 842 mW cm^{-2} at 800 °C, respectively. These results suggest that CG30 is a promising cathode material for use in IT-SOFCs.

Acknowledgments

This work was supported by Priority Research Centers Program (2011-0031407), the Pioneer Research Center Program (2010-0019469), and Program to Solve Climate Changes (NRF-2010-C1AAA001-2010-0029031) through the National Research Foundation of Korea (NRF) funded by the Ministry of Education, Science and Technology.

REFERENCES

[1] Lü S, Long G, Ji Y, Meng X, Sun C. Characterization of $SmBaCoFeO_{5+\delta}$–$Ce_{0.9}Gd_{0.1}O_{1.95}$ composite cathodes for

intermediate-temperature solid oxide fuel cells. Int J Hydrogen Energy 2010;35:7930–5.
[2] Lee SJ, Muralidharan P, Jo SH, Kim DK. Composite cathode for IT-SOFC: Sr-doped lanthanum cuprate and Gd-doped ceria. Electrochem Commun 2010;12:808–11.
[3] Chen D, Ran R, Shao Z. Assessment of $PrBaCo_2O_{5+\delta}$ + $Sm_{0.2}Ce_{0.8}O_{1.9}$ composites prepared by physical mixing as electrodes of solid oxide fuel cells. J Power Sources 2010;195:7187–95.
[4] Lee SJ, Kim DS, Muralidharan P, Jo SH, Kim DK. Improved electrochemical performance and thermal compatibility of Fe- and Cu-doped $SmBaCoFeO_{5+\delta}$–$Ce_{0.9}Gd_{0.1}O_{1.95}$ composite cathodes for intermediate-temperature solid oxide fuel cells. J Power Sources 2011;196:3095–8.
[5] Nagasawa K, Daviero-Minaud S, Preux N, Rolle A, Roussel P, Nakatsugawa H, et al. $Ca_3Co_4O_{9-\delta}$: a thermoelectric material for SOFC cathode. Chem Mater 2009;21:4738–45.
[6] Fu YP. Electrochemical performance of $La_{0.9}Sr_{0.1}Co_{0.8}Ni_{0.2}O_{3-\delta}$–$Ce_{0.8}Sm_{0.2}O_{1.9}$ composite cathode for solid oxide fuel cells. Int J Hydrogen Energy 2011;36:5574–80.
[7] Zhu CJ, Liu XM, Xu D, Wang DJ, Yan DT, Pei L, et al. Electrochemical performance of $Pr_{0.7}Sr_{0.3}Co_{0.9}Cu_{0.1}O_{3-\delta}$–$Ce_{0.8}Sm_{0.2}O_{1.9}$ composite cathodes in intermediate-temperature solid oxide fuel cells. J Power Sources 2008;185:212–6.
[8] Murray EP, Sever MJ, Barnett SA. Electrochemical performance of (La, Sr)(Co, Fe)O_3–(Ce, Gd)O_3 composite cathodes. Solid State Ion 2002;148:27–34.
[9] Shao Z, Haile SM. A high-performance cathode for the next generation of solid-oxide fuel cells. Nature 2004;431:170–3.
[10] Hou SE, Alonso JA, Goodenough JB. Co-free, iron perovskites as cathode materials for intermediate-temperature solid oxide fuel cells. J Power Sources 2010;195:280–4.
[11] Ling Y, Zhao L, Lin B, Dong Y, Zhang X, Meng G, et al. Investigation of cobalt-free cathode material $Sm_{0.5}Sr_{0.5}Fe_{0.8}Cu_{0.2}O_{3-\delta}$ for intermediate temperature solid oxide fuel cells. Int J Hydrogen Energy 2010;35:6905–10.
[12] Ling Y, Yu J, Lin B, Zhang X, Zhao L, Liu X. A cobalt-free $Sm_{0.5}Sr_{0.5}Fe_{0.8}Cu_{0.2}O_{3-\delta}$–$Ce_{0.8}Sm_{0.2}O_{2-\delta}$ composite cathode for proton-conducting solid oxide fuel cells. J Power Sources 2011;196:2631–4.
[13] Zhou Q, Zhang L, He T. Cobalt-free cathode material $SrFe_{0.9}Nb_{0.1}O_{3-\delta}$ for intermediate-temperature solid oxide fuel cells. Electrochem Commun 2010;12:285–7.
[14] Ralph M, Rossignol C, Kumar R. Cathode materials for reduced-temperature SOFCs. J Electrochem Soc 2003;150: A1518–22.
[15] Niu Y, Zhou W, Sunarso J, Ge L, Zhu Z, Shao Z. High performance cobalt-free perovskite cathode for intermediate temperature solid oxide fuel cells. J Mater Chem 2010;20:9619–22.
[16] Azzoni CB, Mozzati MC, Massarotti V, Capsoni D, Bini M. New insights into the magnetic properties of the Ca_2FeO_5 ferrite. Solid State Ion 2007;9:515–20.
[17] Shaula AL, Pivak YV, Waerenborgh JC, Gaczyñski P, Yarechenko AA, Kharton VV. Ionic conductivity of brownmillerite-type calcium ferrite under oxidizing conditions. Solid State Ion 2006;177:2923–30.
[18] Hirabayashi D, Yoshikawa T, Mochizuki K, Suzuki K, Sakai Y. Formation of brownmillerite type calcium ferrite ($Ca_2Fe_2O_5$) and catalytic properties in propylene combustion. Catal Lett 2006;110:155–60.
[19] Li Q, Sun L, Huo L, Zhao H, Grenier JC. Electrode properties of Co-doped $Ca_2Fe_2O_5$ as new cathode materials for intermediate-temperature SOFCs. Int J Hydrogen Energy 2010;35:9151–7.
[20] Berastegi P, Eriksson SG, Hull S. A neutron diffraction study of the temperature dependence of $Ca_2Fe_2O_5$. Mater Res Bull 1999;34:303–14.
[21] Stølen S, Mohn CE, Ravindran P, Allan NL. Topography of the potential energy hypersurface and criteria for fast-ion conduction in perovskite-related $A_2B_2O_5$ oxides. J Phys Chem B 2009;109:12362–5.
[22] Isupova LA, Tsybulya SV, Kryukova GN, Budneva AA, Paukshtis EA, Litvak GS, et al. Mechanochemical synthesis and catalytic properties of the calcium ferrite $Ca_2Fe_2O_5$. Kinet Catal 2002;43:132–9.
[23] Yang Y, Cao Z, Jiang Y, Liu L, Sun Y. Photoinduced structural transformation of $SrFeO_3$ and $Ca_2Fe_2O_5$ during photodegradation of methyl orange. Mater Sci Eng B 2006; 132:311–4.
[24] Asenath-Smith E, Lokuhewa IN, Misture ST, Edwards DD. p-type thermoelectric properties of the oxygen-deficient perovskite $Ca_2Fe_2O_5$ in the brownmillerite structure. J Solid State Chem 2010;183:1670–7.
[25] Sharma N, Shaju KM, Subba Rao GV, Chowdari BVR. Mixed oxides $Ca_2Fe_2O_5$ and $Ca_2Co_2O_5$ as anode materials for Li-ion batteries. Electrochim Acta 2004;49:1035–43.
[26] Gazzarri JI, Kesler O. Non-destructive delamination detection in solid oxide fuel cells. J Power Sources 2007;167:430–41.
[27] Jacobson AJ. Materials for solid oxide fuel cells. Chem Mater 2010;22:660–74.
[28] Kim JH, Cassidy M, Irvine JTS, Bae JM. Advanced electrochemical properties of $LnBa_{0.5}Sr_{0.5}Co_2O_{5+\delta}$ (Ln = Pr, Sm, and Gd) as cathode materials for IT-SOFC. J Electrochem Soc 2009;156:B682–9.
[29] Jo SH, Muralidharan P, Kim DK. Enhancement of electrochemical performance and thermal compatibility of $GdBaCo_{2/3}Fe_{2/3}O_{5+\delta}$ cathode on $Ce_{1.9}Gd_{0.1}O_{1.95}$ electrolyte for IT-SOFCs. Electrochem Commun 2009;11:2085–8.
[30] Leng Y, Chan SH, Liu Q. Development of LSCF-GDC composite cathodes for low-temperature solid oxide fuel cells with thin film GDC electrolyte. Int J Hydrogen Energy 2008;33:3808–17.
[31] Tao Z, Bi L, Zhu Z, Liu W. Novel cobalt-free cathode materials $BaCe_\chi Fe_{1-\chi}O_{3-\delta}$ for proton-conducting solid oxide fuel cells. J Power Sources 2009;194:801–4.